

Weak-Coupling Model for ^{212}Pb and $^{204}\text{Pb}^\dagger$

C. M. Ko and T. T. S. Kuo

Department of Physics, State University of New York, Stony Brook, New York 11790

and

J. B. McGrory*

Physics Division, Oak Ridge National Laboratory, Oak Ridge, Tennessee 37830

(Received 16 August 1973)

The weak-coupling model is applied to the study of the low-lying states of ^{212}Pb and ^{204}Pb . We first obtain the phonon states of ^{210}Pb and ^{206}Pb by shell-model calculations. The states of ^{212}Pb (^{204}Pb) are then obtained by solving the eigenvalue problem in a truncated Hilbert space consisting of a small number of basis vectors, each of which is a product of two phonon states of ^{210}Pb (^{206}Pb). A canonical transformation is used to orthonormalize these two-phonon basis vectors. The energies as well as the wave functions of many low-lying states of ^{212}Pb (^{204}Pb) given by the exact shell-model calculations are reproduced surprisingly well by the weak-coupling model where only three or four low-lying ^{210}Pb (^{206}Pb) phonons are included.

[NUCLEAR STRUCTURE ^{212}Pb , ^{204}Pb ; energies and wave functions calculated in terms of the ^{210}Pb and ^{206}Pb phonons.]

1. INTRODUCTION

The nuclear shell model has proven to be an extremely useful tool in the study of nuclear structure from a microscopic point of view. There are two important difficulties with the conventional shell model. First, as the number of particles and/or the number of single-particle orbits in the active model space increase, the dimensions of resultant matrices which must be calculated and diagonalized become prohibitively large. Second, even when one can handle the relatively large matrices, the eigenvectors which are interpreted as nuclear wave functions are very complex. Consequently, it is difficult to make a simple interpretation of the wave functions.

Because the shell model is such a useful tool, it would be very useful to find simple approximations to large shell-model calculations. Ideally, one would find a Hilbert space of which the dimension is much smaller than the complete shell-model space, such that the eigenvalues of the original Hamiltonian in this smaller space reproduce the eigenvalues in the large space, and the small-dimension eigenvectors have large overlaps with the full shell-model wave functions. This is the aim of the so-called "weak coupling" schemes and their generalizations.¹⁻⁵ An extensive review of such calculations has been presented by Arima and Hamamoto.⁴ The general idea is to view the complete shell-model Hilbert space of n particles as the product of two spaces of m_1 and m_2 particles

($n = m_1 + m_2$), and to look for truncations in the spaces m_1 and m_2 so that the product space generated from the two truncated subspaces has strong overlap with the space spanned by the low-lying eigenstates in the n -particles space. One example of such a scheme is discussed by Wong and Zuker.⁵ They considered nuclei in the s - d shell. The conventional shell-model calculation of ^{20}Ne consists of diagonalizing a one-body and a two-body effective residual interaction in the space of four particles distributed over the $d_{5/2}$, $s_{1/2}$, and $d_{3/2}$ orbits. Wong and Zuker found that the low-lying eigenstates of ^{20}Ne could be well described as the result of coupling together only few low-lying eigenstates in ^{18}F . An extreme example of a weak-coupling scheme is the so-called pairing-vibrational scheme,⁶ where only one basis state of each J is included in the two-particle Hilbert space, and the states in the nucleus with $2n$ active particles are simply the products of n of these two-particle states. Obviously as one includes more and more of the states in the smaller spaces, one approaches the exact shell-model calculation.

In this paper, we present the results of a study of a generalized weak-coupling scheme for the lead isotopes ^{212}Pb and ^{204}Pb . We consider the states of ^{212}Pb as the products of low-lying eigenstates in ^{210}Pb , and similarly, ^{204}Pb states are treated as products of ^{206}Pb eigenstates. For these cases, we can handle fairly large exact shell-model calculations, and thus can compare the weak-coupling results with the exact results. In our for-

mulation, we can handle an arbitrary number of two-particle (hole) "phonons," so we can study the calculations as a function of the number of phonons we include in the weak-coupling space. The calculation is formulated in a second-quantized representation so that the Pauli principle is treated exactly. We shall find that the weak-coupling ap-

proach is extremely useful in these Pb isotopes. We also show that for a certain set of states, the pairing-vibration model is a very good one.

In Sec. 2 we discuss the method of calculation in some detail. The numerical results are presented and discussed in Sec. 3. A summary of the calculation is presented in Sec. 4.

2. METHOD OF CALCULATION

In the weak coupling-model used here, the states in the nucleus ^{212}Pb (^{204}Pb) are considered as products of two-particle (two-hole) eigenstates in ^{210}Pb (^{206}Pb) nuclei, in the sense that the four valence particles (holes) outside (inside) the ^{208}Pb core are considered linear combinations of products of two two-particle (two-hole) systems, where each two-particle (two-hole) system is taken as the phonon states (eigenstates) of ^{210}Pb (^{206}Pb). Let us denote the normalized two-particle (two-hole) phonon states by $|\alpha\rangle$. Then the basis states for the four valence particles (holes) of ^{212}Pb (^{204}Pb) are constructed from coupling two phonon states. Since the two-phonon states are usually not orthonormal to each other, we have used the canonical transformation⁷ to construct a set of orthonormal states $|m\rangle$ out of the two-phonon states $|\alpha_1\alpha_2\rangle$. This involves the diagonalization of the overlap matrix of the two-phonon states. If we write $|\alpha\rangle$ in terms of the normalized antisymmetric two-particle (hole) states as

$$|\alpha\rangle = \sum_{(ab)} \frac{A_{\alpha}^{(ab)}}{(1+\delta_{ab})^{1/2}} |(ab)J_{\alpha}\rangle, \quad (1)$$

then the overlap matrix can be expressed as

$$\begin{aligned} \langle\langle(\alpha_1\alpha_2)J|(\alpha_3\alpha_4)J\rangle\rangle &= \sum_{(ab)} \sum_{(cd)} \sum_{(ef)} \sum_{(gh)} \frac{A_{\alpha_1}^{(ab)}}{(1+\delta_{ab})^{1/2}} \frac{A_{\alpha_2}^{(cd)}}{(1+\delta_{cd})^{1/2}} \frac{A_{\alpha_3}^{(ef)}}{(1+\delta_{ef})^{1/2}} \frac{A_{\alpha_4}^{(gh)}}{(1+\delta_{gh})^{1/2}} \\ &\quad \times \langle\langle(ab)^{J_1}(cd)^{J_2}J|(ef)^{J_3}(gh)^{J_4}J\rangle\rangle, \end{aligned} \quad (2)$$

where the four-particle overlap matrix element is given by

$$\begin{aligned} \langle\langle(ab)^{J_1}(cd)^{J_2}J|(ef)^{J_3}(gh)^{J_4}J\rangle\rangle &= \delta_{J_1 J_3} \delta_{J_2 J_4} \langle\langle(ab)J_1|(ef)J_3\rangle\rangle \langle\langle(cd)J_2|(gh)J_4\rangle\rangle + \delta_{J_1 J_4} \delta_{J_2 J_3} \langle\langle(ab)J_1|(gh)J_4\rangle\rangle \langle\langle(cd)J_2|(ef)J_3\rangle\rangle (-1)^{J_3+J_4-J} \\ &\quad - (\hat{J}_1 \hat{J}_2 \hat{J}_3 \hat{J}_4)^{1/2} \sum_{r \neq s} \sum_{u \neq v} \begin{pmatrix} r & s & J_1 \\ u & v & J_2 \\ J_3 & J_4 & J \end{pmatrix} F(rs)F(uv) \langle\langle(ru)J_3|(ef)J_3\rangle\rangle \langle\langle(sv)J_4|(gh)J_4\rangle\rangle, \end{aligned} \quad (3)$$

where the sum over $r \neq s$ means r can be either a or b , as can s , but under the constraint $r \neq s$. For example if $(ab) = (12)$, then (rs) is (12) and (21) ; similarly for the sum over $u \neq v$. In the above, we have used the following abbreviated notations:

$$\begin{aligned} \delta_{ab} &= 1 \quad \text{if } j_a = j_b \\ &= 0 \quad \text{if } j_a \neq j_b, \\ \hat{J} &= 2J+1, \\ F(rs) &= 1 \quad \text{if } r=a, s=b \\ &= (-1)^{1+j_a+j_b-J_1} \quad \text{if } r=b, s=a, \\ \langle\langle(ab)J_2|(cd)J_2\rangle\rangle &= \delta_{ac}\delta_{bd} - (-1)^{j_c+j_d-J_2} \delta_{ad}\delta_{bc}. \end{aligned} \quad (4)$$

Note that the state $|(ab)J\rangle$ is antisymmetrized, but is normalized only when $j_a \neq j_b$. The above expressions have been derived in a second-quantized formalism, and hence the states $|\alpha_1\alpha_2\rangle$ are fully

antisymmetrized. The state $|\alpha\rangle$ of Eq. (1) is normalized, but the states $|\langle\langle\alpha_1\alpha_2\rangle\rangle$ are not yet normalized. Using Eq. (3) they can be easily normalized. We denote the normalized two-phonon states by $|\langle\langle\alpha_1\alpha_2\rangle\rangle$, namely

$$\begin{aligned} |\langle\langle\alpha_1\alpha_2\rangle\rangle &= N_{12J}^{1/2} |(\alpha_1\alpha_2)J\rangle \\ N_{12J} &= \langle\langle\langle\langle\alpha_1\alpha_2\rangle\rangle | \langle\langle\alpha_1\alpha_2\rangle\rangle\rangle^{-1}. \end{aligned} \quad (5)$$

Let the eigenvalues and eigenvectors of the overlap matrix of the normalized two-phonon states $|\langle\langle\alpha_1\alpha_2\rangle\rangle$ be λ_m and

$$\phi_m = \sum_{(\alpha_1\alpha_2)} B_m^{\langle\langle\alpha_1\alpha_2\rangle\rangle} |(\alpha_1\alpha_2)J\rangle, \quad (6)$$

respectively. Then the set of orthonormalized states $|m\rangle$ is given by

$$|m\rangle = \sum_{(\alpha_1\alpha_2)} C_m^{\langle\langle\alpha_1\alpha_2\rangle\rangle} |(\alpha_1\alpha_2)J\rangle, \quad (7)$$

where

$$C_m^{(\alpha_1\alpha_2)} = \frac{B_m^{(\alpha_1\alpha_2)}}{\sqrt{\lambda_m}}. \quad (8)$$

Obviously $|m\rangle$ is not defined when $\lambda_m=0$. This problem arises because our two-phonon basis is overcomplete. It can be shown that the eigenvectors of the overlap matrix which have zero eigenvalues are linearly dependent on the eigenvectors with nonzero eigenvalues. One obtains a complete orthonormal basis for the space of two-phonon

states by neglecting those ϕ_m 's which correspond to zero eigenvalues.

Once we have obtained a set of orthonormalized basis states, the eigenvalue problem for ^{212}Pb (^{204}Pb) can be written as

$$\sum_{m'} \langle m|H|m'\rangle b_m^N = E_N b_m^N, \quad (9)$$

where E_N is the energy of ^{212}Pb (^{204}Pb) relative to the ground-state energy of ^{208}Pb . The matrix element

$\langle m|H|m'\rangle$ is equal to

$$\langle m|H|m'\rangle = \sum_{(\alpha_1\alpha_2), (\alpha_3\alpha_4)} C_m^{(\alpha_1\alpha_2)} C_{m'}^{(\alpha_3\alpha_4)} \{ (E_{\alpha_1} + E_{\alpha_2}) [\delta_{\alpha_1\alpha_3} \delta_{\alpha_2\alpha_4} + (-1)^{J_1+J_2-J} \delta_{\alpha_1\alpha_4} \delta_{\alpha_2\alpha_3}] (N_{12J} N_{34J})^{1/2} + \langle (\alpha_1\alpha_2)J|H_0|(\alpha_3\alpha_4)J\rangle_C + \langle (\alpha_1\alpha_2)J|H_1|(\alpha_3\alpha_4)J\rangle_C \}, \quad (10)$$

where the E 's are the phonon energies of ^{210}Pb (^{206}Pb). The matrix element $\langle (\alpha_1\alpha_2)J|H_0|(\alpha_3\alpha_4)J\rangle_C$ can be expressed in terms of part of the four-particle overlap matrix element, i.e.,

$$\langle (\alpha_1\alpha_2)J|H_0|(\alpha_3\alpha_4)J\rangle_C = (N_{12J} N_{34J})^{1/2} \sum_{(ab)} \sum_{(cd)} \sum_{(ef)} \sum_{(gh)} \frac{A_{\alpha_1}^{(ab)}}{(1+\delta_{ab})^{1/2}} \frac{A_{\alpha_2}^{(cd)}}{(1+\delta_{cd})^{1/2}} \frac{A_{\alpha_3}^{(ef)}}{(1+\delta_{ef})^{1/2}} \frac{A_{\alpha_4}^{(gh)}}{(1+\delta_{gh})^{1/2}} \times (\epsilon_a + \epsilon_b + \epsilon_c + \epsilon_d) \langle (ab)^{J_1}(cd)^{J_2}J|(ef)^{J_3}(gh)^{J_4}J\rangle_C, \quad (11)$$

where $\langle \dots \rangle_C$ is the third term in the overlap matrix element given by Eq. (3), and the ϵ 's are the single-particle (hole) energies. The matrix element $\langle (\alpha_1\alpha_2)J|H_1|(\alpha_3\alpha_4)J\rangle_C$ can be written as

$$\langle (\alpha_1\alpha_2)J|H_1|(\alpha_3\alpha_4)J\rangle_C = (N_{12J} N_{34J})^{1/2} \sum_{(ab)} \sum_{(cd)} \sum_{(ef)} \sum_{(gh)} \frac{A_{\alpha_1}^{(ab)}}{(1+\delta_{ab})^{1/2}} \frac{A_{\alpha_2}^{(cd)}}{(1+\delta_{cd})^{1/2}} \frac{A_{\alpha_3}^{(ef)}}{(1+\delta_{ef})^{1/2}} \frac{A_{\alpha_4}^{(gh)}}{(1+\delta_{gh})^{1/2}} \times \langle (ab)^{J_1}(cd)^{J_2}J|H_1|(ef)^{J_3}(gh)^{J_4}J\rangle_C, \quad (12)$$

with

$$\begin{aligned} & \langle (ab)^{J_1}(cd)^{J_2}J|H_1|(ef)^{J_3}(gh)^{J_4}J\rangle_C \\ &= (\hat{J}_1 \hat{J}_2 \hat{J}_3 \hat{J}_4)^{1/2} \left[- \sum_{r \neq s} \sum_{u \neq v} \begin{pmatrix} ab & cd \\ r & s \\ J_3 & J_4 \end{pmatrix} \begin{pmatrix} r & s & J_1 \\ u & v & J_2 \end{pmatrix} F(rs)F(uv) \langle (ru)^{J_3}(sv)^{J_4}J|H_1|(ef)^{J_3}(gh)^{J_4}J\rangle \\ & \quad - \sum_{r' \neq s'} \sum_{u' \neq v'} \begin{pmatrix} ef & gh \\ r' & s' \\ J_1 & J_2 \end{pmatrix} \begin{pmatrix} r' & s' & J_3 \\ u' & v' & J_4 \end{pmatrix} F(r's')F(u'v') \langle (ab)^{J_1}(cd)^{J_2}J|H_1|(r'u')^{J_1}(s'v')^{J_2}J\rangle \\ & \quad + \frac{1}{2} \sum_{r \neq s} \sum_{u \neq v} \sum_{r' \neq s'} \sum_{u' \neq v'} \sum_{J'_1 J'_2} \hat{J}'_1 \hat{J}'_2 \begin{pmatrix} r & s & J_1 \\ u & v & J_2 \\ J'_1 & J'_2 & J \end{pmatrix} \begin{pmatrix} r' & s' & J_3 \\ u' & v' & J_4 \\ J'_1 & J'_2 & J \end{pmatrix} F(rs)F(uv)F(r's')F(u'v') \\ & \quad \times \langle (ru)^{J_1}(sv)^{J_2}J|H_1|(r'u')^{J_1}(s'v')^{J_2}J\rangle \left. \right] \quad (13) \end{aligned}$$

and

$$\begin{aligned} \langle (ru)^{J_1}(sv)^{J_2}J|H_1|(r'u')^{J_1}(s'v')^{J_2}J\rangle &= \langle (ru)J'_1|H_1|(r'u')J'_1\rangle \langle (sv)J'_2|(s'v')J'_2\rangle \\ & \quad + \langle (sv)J'_2|H_1|(s'v')J'_2\rangle \langle (ru)J'_1|(r'u')J'_1\rangle. \quad (14) \end{aligned}$$

In the above, the meanings of various notations are the same as in Eq. (4) except that the $\langle (rs)J'|H_1|(r's')J'\rangle$'s are the effective interaction matrix elements. The subscript C empha-

sizes that only the matrix elements which correspond to the contractions between the two phonons are included. For instance, the matrix elements of the type $\langle \alpha_1|H_1|\alpha_3\rangle$ and $\langle \alpha_2|H_1|\alpha_4\rangle$ are excluded

in Eqs. (12) and (13) because they are contained in E_{α_1} and E_{α_2} of Eq. (10) already.

In this discussion we have ignored the isospin quantum numbers since ^{212}Pb (^{204}Pb) has only neutron valence particles (holes) and therefore the total valence isospin is always 2. Note that the above formulas apply to both ^{212}Pb and ^{204}Pb .

3. RESULTS OF CALCULATIONS

In all these calculations, we use the two-body particle-particle and hole-hole matrix elements developed for this mass region by Herling and Kuo.^{8,9} The matrix elements are derived by reaction matrix techniques from the Hamada-Johnston potential. We include the contributions from the bare interaction and from the core-polarization diagram. The structure of ^{212}Pb has been studied in terms of two model spaces. Model space I includes only two single-particle orbits, the $1g_{9/2}$ and the $0i_{11/2}$. In model space II, we include the five lowest neutron orbits outside ^{208}Pb , i.e., $1g_{9/2}$, $0i_{11/2}$, $0j_{15/2}$, $2d_{5/2}$, and $3s_{1/2}$ with respective single-particle energies -3.94 , -3.15 , -2.53 , -2.36 , and -1.91 MeV which are the observed energies in ^{209}Pb , the same as those used by Herling and Kuo.⁸

TABLE I. Phonon states of ^{210}Pb (model space I).

J^π	Energy	$(0i_{11/2})^2$	$(0i_{11/2})(1g_{9/2})$	$(1g_{9/2})^2$
0_1^+	-8.546	0.2932	0.0	0.9560
2_1^+	-8.175	0.0222	-0.0316	0.9993
4_1^+	-7.977	0.0251	-0.0175	0.9995

A. ^{212}Pb in Model Space I

In the two-shell model space I, we first obtain the phonon states of ^{210}Pb from the conventional shell-model calculation with the above-mentioned effective interaction. The excitation energy spectra of the two-shell phonon states is shown in column one of Fig. 1. We would not expect very precise agreement with the observed spectrum of ^{210}Pb because the Herling and Kuo matrix elements are designed for a model space of seven orbits. Since we are interested in the low-lying states of ^{212}Pb , we first consider a weak-coupling model based on the lowest 0_1^+ , 2_1^+ , and 4_1^+ phonons of ^{210}Pb . The wave functions of these two-particle phonons are shown in Table I. The Hilbert spaces associat-

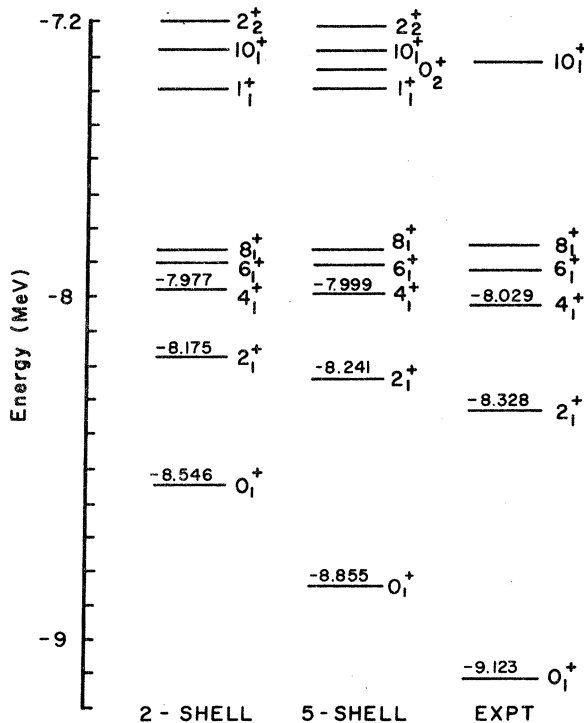


FIG. 1. Energy levels of ^{210}Pb .

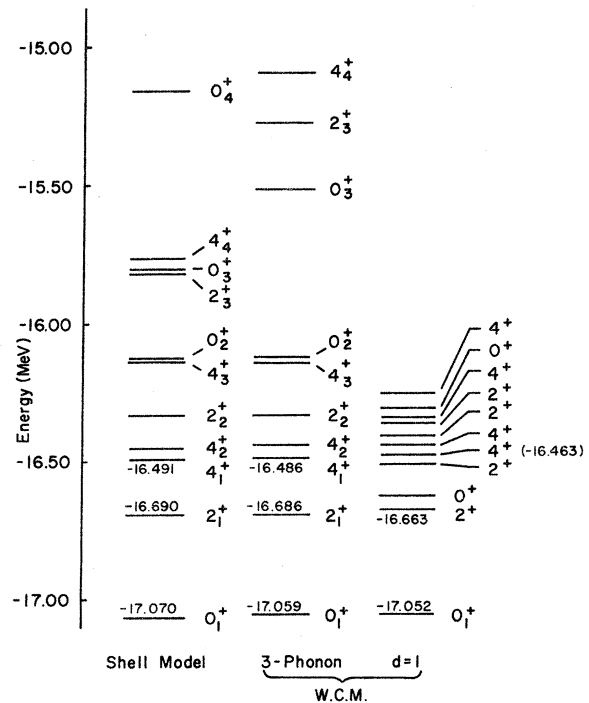


FIG. 2. Energy levels of ^{212}Pb (model space I).

TABLE II. 0^+ states of ^{212}Pb (model space I).

J^π	Energy	$(0_1^+ 0_1^+)$	$(2_1^+ 2_1^+)$	$(4_1^+ 4_1^+)$
0_1^+	-17.059	-0.8666	0.1254	0.0796
0_2^+	-16.117	0.0017	0.5131	-0.8445

ed with the 0^+ , 2^+ , and 4^+ states of ^{212}Pb have basis states $(|0_1^+ 0_1^+\rangle, |2_1^+ 2_1^+\rangle, |4_1^+ 4_1^+\rangle)$; $(|0_1^+ 2_1^+\rangle, |2_1^+ 2_1^+\rangle, |2_1^+ 4_1^+\rangle, |4_1^+ 4_1^+\rangle)$; and $(|0_1^+ 4_1^+\rangle, |2_1^+ 2_1^+\rangle, |2_1^+ 4_1^+\rangle, |4_1^+ 4_1^+\rangle)$, respectively. Using the expressions discussed before, we obtain the weak-coupling states of ^{212}Pb in this truncated basis. The results are shown in Fig. 2 labeled W.C.M. (weak-coupling model). The complete two-orbit shell-model result is shown in column 1. We also show in Fig. 2 the results of the simplest weak-coupling model labeled $d=1$, in which we ignore mixing between basis states. By this we mean that we have calculated the energy of each weak-coupling state $|(J_1 J_2)J\rangle$ as the sum of the J_1 and J_2 phonon energies plus the energy of interaction between the two phonons. This result is analogous to the simplest pairing-vibration-model result. For the lowest 0^+ , 2^+ , and 4^+ states in ^{212}Pb , this model gives excellent agreement with the exact calculation. Much of the rest of the $d=1$ spectrum looks too compressed. Part of this compression comes from the fact that we have ignored the nonorthogonality of the two-phonon states in calculating the $d=1$ spectrum. This problem is treated correctly in the three-phonon weak-coupling model, and we see that in this case there is excellent agreement with the exact shell-model result for the lowest seven states, i.e., 0_1^+ , 2_1^+ , 4_1^+ , 4_2^+ , 2_2^+ , 4_3^+ , and 0_2^+ . The good agreement is not only true for the energies of these states. It is also true for the wave functions, which are shown in Tables II-IV. [Note that in these tables, the wave functions are expressed in terms of the overcomplete set of the normalized two-phonon states $|(J_1 J_2)J\rangle$. This accounts for the apparent lack of normalization and orthogonalization in the tables.]

The overlap of the wave function from the weak-coupling model and the corresponding shell-model wave function is better than 0.99 for all these states. Although the evaluation of the overlap is straightforward, it usually requires a large amount

TABLE III. 2^+ states of ^{212}Pb (model space I).

J^π	Energy	$(0_1^+ 2_1^+)$	$(2_1^+ 2_1^+)$	$(2_1^+ 4_1^+)$	$(4_1^+ 4_1^+)$
2_1^+	-16.686	0.6745	0.2347	-0.2742	0.0483
2_2^+	-16.332	0.0000	-0.5442	-0.1571	0.4420

TABLE IV. 4^+ states of ^{212}Pb (model space I).

J^π	Energy	$(0_1^+ 4_1^+)$	$(2_1^+ 2_1^+)$	$(2_1^+ 4_1^+)$	$(4_1^+ 4_1^+)$
4_1^+	-16.486	0.6917	-0.5398	0.3938	-0.2470
4_2^+	-16.438	-0.0552	-0.2470	-0.6635	0.4939
4_3^+	-16.128	-0.0367	0.5258	0.1959	1.0788

of computation. This is because the shell-model wave function generally has a large number of components and employs an angular momentum coupling scheme which is different from that of the weak-coupling model. We outline in the Appendix the procedure for evaluating these wave-function overlaps. We point out above that the 0_1^+ , 2_1^+ , and 4_1^+ states are reasonably described by the simple coupling scheme, which implies that these states are associated with very simple structures. Actually, for the wave functions of these states in the weak-coupling model, the overlaps of 0_1^+ , 2_1^+ , and 4_1^+ states of ^{212}Pb with $(0_1^+ 0_1^+)$, $(0_1^+ 2_1^+)$, and $(0_1^+ 4_1^+)$ are 0.999, 0.992, and 0.991, respectively. In passing, we remark that the dimensions associated with the shell-model Hamiltonian matrices are 12, 31, and 45, respectively, for the 0^+ , 2^+ , and 4^+ states,

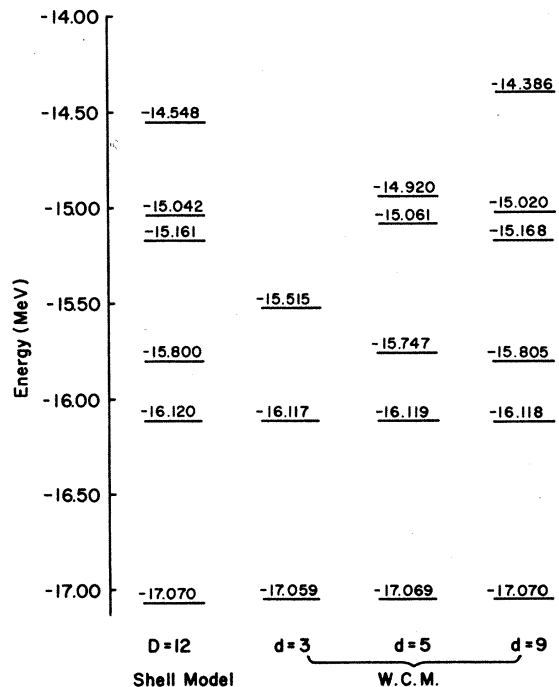


FIG. 3. $J=0^+$ energy levels of ^{212}Pb (model space I). The dimensionality for the shell model and the weak-coupling model is denoted by D and d , respectively.

TABLE VI. 0^+ states of ^{212}Pb (model space II).

J^π	Energy	$(0_1^+ 0_1^+)$	$(2_1^+ 2_1^+)$	$(4_1^+ 4_1^+)$
0_1^+	-17.601	-0.9443	0.0661	0.0540
0_2^+	-16.137	0.2345	-0.2426	0.9821

pling model and compared with the shell-model results obtained in the five-orbit model space. As shown in Fig. 4, the shell-model 0_1^+ , 2_1^+ , 4_1^+ , 4_2^+ , and 2_3^+ states of ^{212}Pb are reproduced quite well by this three-phonon W.C.M. calculation. The W.C.M. results are obtained with Hamiltonian matrices of dimensions 3 for 0^+ states, 4 for 2^+ states, and 3 for 4^+ states, but the respective dimensions in the shell model are 72, 253, and 380. The reduction in dimension is indeed very impressive.

There are additional shell-model states which are not accounted for by the three-phonon W.C.M. calculation, as seen in Fig. 4. To see whether these states can be reproduced by including more ^{210}Pb phonons, the spectrum for the 0^+ states are calculated in the weak-coupling spaces which include the lowest 3, 6, and 12 two-phonon states. The results are shown in Fig. 5 where the W.C.M. Hamiltonian matrices have dimensions 3, 6, and 12, respectively. We see that the ground-state energy is little effected as the dimension increases. Clearly more shell-model states are reproduced when more two-phonon states are included. In the $d=12$ case, the lowest five states are indeed all in good agreement with the corresponding shell-model states. Note that the dimension of $d=12$ is still a factor of 6 smaller than the corresponding shell-model dimension. In the last column of Fig. 4, we show the results for the simplest weak-coupling model where only the 0_1^+ , 2_1^+ , and 4_1^+ ^{210}Pb phonons are included and the mixing between the two-phonon basis states are ignored as discussed in the preceding section. We see that even in this case the lowest three states are in good agreement with the corresponding shell-model states.

To identify which W.C.M. state is associated with which shell-model state, we must compare both the energies and the wave functions. To this point we have compared only energies. We show in Ta-

TABLE VII. 2^+ states of ^{212}Pb (model space II).

J^π	Energy	$(0_1^+ 2_1^+)$	$(2_1^+ 2_1^+)$	$(2_1^+ 4_1^+)$	$(4_1^+ 4_1^+)$
2_1^+	-16.981	0.774	0.215	-0.211	0.048
2_2^+	-16.431	-0.019	-0.600	-0.274	0.333
2_3^+	-15.640	-1.231	0.962	-1.144	0.182

TABLE VIII. 4^+ states of ^{212}Pb (model space II).

J^π	Energy	$(0_1^+ 4_1^+)$	$(2_1^+ 2_1^+)$	$(2_1^+ 4_1^+)$
4_1^+	-16.709	-0.863	0.251	-0.150
4_2^+	-16.510	0.176	0.614	0.543
4_3^+	-15.690	-0.836	-1.190	1.183

bles VI–VIII some 0^+ , 2^+ , and 4^+ W.C.M. wave functions expressed in terms of the two-phonon states which are normalized but not orthogonalized. The W.C.M. wave functions usually have very simple structures. For instance the 0_1^+ , 2_1^+ , and 4_1^+ states shown in these tables have overlaps of 0.998, 0.980, and 0.983 with the two-phonon states $|0_1^+ 0_1^+\rangle$, $|0_1^+ 2_1^+\rangle$, and $|0_1^+ 4_1^+\rangle$, respectively. In Table IX we show the overlaps between the shell-model and the W.C.M. 0_1^+ , 0_2^+ , and 0_3^+ states of Fig. 4. It is clearly seen from these overlaps that the W.C.M. 0_2^+ state matches much better with the shell-model 0_3^+ state than the shell-model 0_2^+ state. This is consistent to what is shown in Fig. 5, namely the $d=3$ state at -16.137 MeV does not change appreciably as d increases from 3 to 12. But the $d=3$ state at -15.827 MeV gradually moves across the -16.137 -MeV state and approaches the shell-model -16.314 -MeV state.

The overlaps between the 2^+ and 4^+ W.C.M. and shell-model states of Fig. 4 are shown in Table X. Our results indicate strongly that when the W.C.M. and shell-model energies are in good agreement the corresponding wave functions are also in good agreement.

C. ^{204}Pb

For ^{204}Pb , the model space consists of six hole orbits. They are $0h_{9/2}$, $1f_{7/2}$, $0i_{13/2}$, $2p_{3/2}$, $1f_{5/2}$, and $2p_{1/2}$ with respective energies 10.85, 9.72, 9.01, 8.27, 7.95, and 7.38 MeV.⁹ The low-lying states of ^{204}Pb should be dominated by configurations with $p_{1/2}$ and $p_{3/2}$ holes. These are low-spin and thus low-degeneracy orbits. One would expect

TABLE IX. Overlaps of the W.C.M. wave functions with the shell-model wave functions for the 0^+ states of ^{212}Pb shown in Fig. 4.

Shell model	Weak-coupling model (W.C.M.)		
	0_1^+	0_2^+	0_3^+
0_1^+	0.992	0.007	0.017
0_2^+	0.029	0.164	0.832
0_3^+	0.012	0.975	0.143

TABLE X. Overlaps of the W.C.M. wave functions with the shell-model wave functions for the 2^+ and 4^+ states of ^{212}Pb shown in Fig. 4.

Shell model	Weak-coupling model (W.C.M.)			
	2_1^+	2_2^+	4_1^+	4_2^+
2_1^+	0.990	0.011		
2_2^+	0.015	0.991		
4_1^+			0.972	0.123
4_2^+			0.158	0.925

the Pauli effects to be strong and thus that the W.C.M. would not work as well for ^{204}Pb as for ^{212}Pb . Hence it is of even more interest to investigate the accuracy of the W.C.M. for ^{204}Pb than for ^{212}Pb .

The two-hole phonon states of ^{206}Pb are first obtained by shell-model calculations. The phonon spectrum is shown in Fig. 6. Since our purpose here is primarily to study how the lowest shell-model states can be reproduced in the weak-coupling model, we choose, for the time being, only the lowest four even angular momentum phonon states of ^{206}Pb ; the 0_1^+ , 2_1^+ , 0_2^+ , and 2_2^+ states. Their wave functions are shown in Table XI. Then

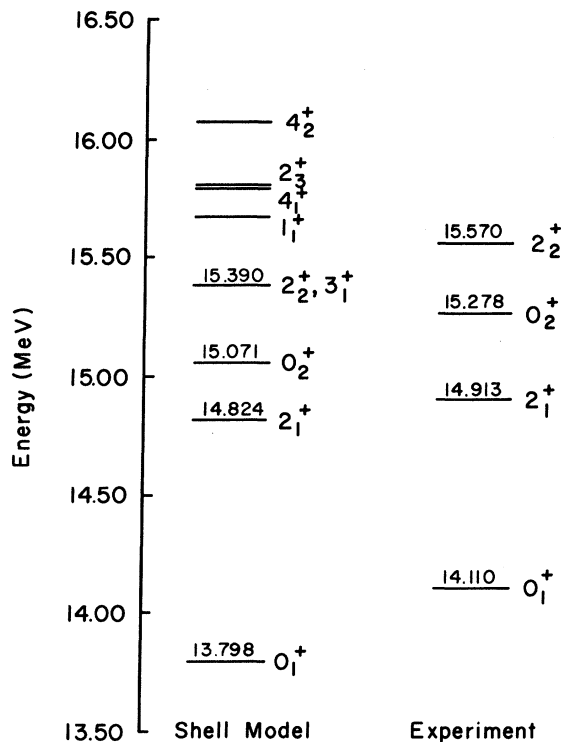


FIG. 6. Energy levels of ^{206}Pb .

TABLE XI. Phonon states of ^{206}Pb . The wave functions are expressed in terms of the two-hole states labeled by $(j_a j_b)$. The numerals 1 to 6 represent the $0h_{9/2}$, $1f_{7/2}$, $1f_{5/2}$, $2p_{3/2}$, $2p_{1/2}$, and $0i_{13/2}$ orbits, respectively.

$(j_a j_b)$	J^π Energy	0_1^+	0_2^+	2_1^+	2_2^+
		13.798	15.071	14.824	15.390
1 1		-0.1734	-0.1229	-0.0554	-0.0089
2 2		-0.2379	-0.1829	-0.0845	-0.0063
3 3		-0.4738	-0.6193	-0.2779	-0.0708
4 4		-0.3829	-0.0368	-0.1438	-0.1755
5 5		-0.6574	0.7030		
6 6		0.3319	0.2691	0.1423	0.0011
1 2				0.0171	0.0036
1 3				-0.1111	0.0037
2 3				-0.0822	0.0018
2 4				-0.1797	0.0229
3 4				0.1639	-0.0187
3 5				-0.7455	0.5777
4 5				-0.4871	-0.7934

the two-phonon basis states for 0^+ and 2^+ states of ^{204}Pb are constructed; they are, respectively, $(|0_1^+0_1^+\rangle, |0_1^+0_2^+\rangle, |2_1^+2_1^+\rangle)$ and $(|0_1^+2_1^+\rangle, |0_1^+2_2^+\rangle, |2_1^+2_1^+\rangle)$. As before, we show in Fig. 7 the levels obtained from the weak-coupling model $d=3$, the shell model, and the simple coupling scheme $d=1$. We see that only the 0_1^+ and 2_1^+ states obtained from the

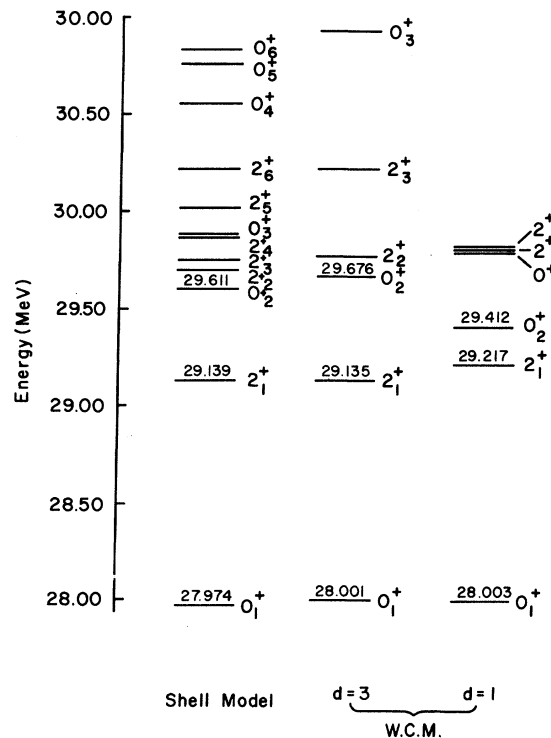


FIG. 7. Energy levels of ^{204}Pb .

TABLE XII. 0^+ and 2^+ states of ^{204}Pb . The wave functions are expressed in terms of the two-phonon states which are normalized but not orthogonalized.

J^π	Energy	$(0_1^+ 0_1^+)$	$(0_1^+ 0_2^+)$	$(2_1^+ 2_1^+)$	$(0_1^+ 2_1^+)$	$(0_1^+ 2_2^+)$
0_1^+	28.001	-0.9742	-0.0309	0.0235		
0_2^+	29.676	0.3212	-1.0311	-0.1757		
2_1^+	29.135			0.1387	-0.9079	0.2757
2_2^+	29.779			0.5468	0.0507	-0.8253
2_3^+	30.198			0.9198	0.5800	0.4953

$d=1$ scheme are reasonable. In the $d=3$ weak-coupling model, five of the six low-lying states have correspondences in the shell model; these states are 0_1^+ , 2_1^+ , 0_2^+ , 2_3^+ , and 2_6^+ . The wave functions of these states are shown in Table XII. The 0_1^+ and 2_1^+ states have 1.000 and 0.954 overlaps with the two-phonon states $|0_1^+ 0_1^+\rangle$ and $|0_1^+ 2_1^+\rangle$, respectively. The other 0^+ state comes a little too high in energy. There are many low-lying shell-model states not reproduced in the $d=3$ model. To reproduce them, it is necessary to extend the dimensions of the weak-coupling model. We have found that the 0_3^+ and 0_4^+ states are reproduced if we include three more two-phonon basis states $|2_1^+ 2_2^+\rangle$, $|0_2^+ 0_2^+\rangle$, and $|2_2^+ 2_2^+\rangle$. But no more 2^+ states could be reproduced even if two-phonon basis states like $|2_1^+ 2_2^+\rangle$ and $|2_2^+ 2_2^+\rangle$ are included in the weak-coupling space. For these states we probably need to take into consideration more low-lying phonon states. However, the good agreement for the lowest states is indeed encouraging, considering the small dimension of the space, since the exact shell-model spaces for the 0^+ and 2^+ states have 113 and 418 basis states, respectively.

The agreement between the W.C.M. wave functions and the corresponding shell-model wave func-

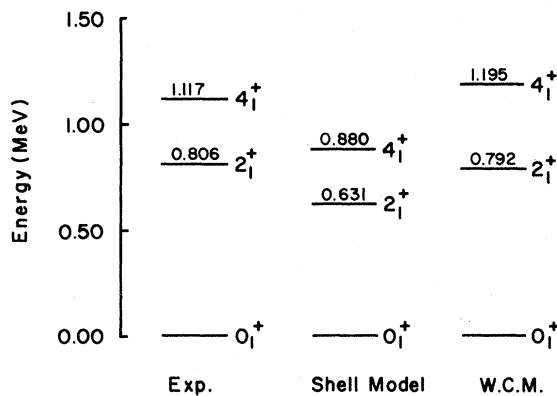


FIG. 8. Excitation spectrum of ^{212}Pb . The experimental phonon energies are used in the W. C. M.

TABLE XIII. Overlaps of the W.C.M. wave functions with the shell-model wave functions for the 0^+ states of ^{204}Pb shown in Fig. 7.

Shell model	Weak-coupling model (W.C.M.)	
	0_1^+	0_2^+
0_1^+	0.990	0.013
0_2^+	0.019	0.896

tions is similar to what we have found for ^{212}Pb . Namely, if the energies are in good agreement, so are the wave functions. To illustrate, we give the wave-function overlaps for the 0_1^+ and 0_2^+ states of ^{204}Pb in Table XIII.

D. Results with Experimental Phonon Energies

In Eq. (10) the phonon energies E_{α_1} and E_{α_2} appear explicitly in the Hamiltonian matrix elements in the weak-coupling model. In the folded diagram formalism¹⁰ the nucleus ^{212}Pb (^{204}Pb) can be decomposed into two ^{210}Pb (^{206}Pb) building blocks or phonons with interactions between them. In fact it can be shown that the phonon energy is the total energy of ^{210}Pb (^{204}Pb) measured from the ground-state energy of ^{208}Pb . These energies can be taken from experiments. It is then possible for us to study the spectra of ^{212}Pb and ^{204}Pb using the experimentally observed phonon energies of ^{210}Pb and ^{206}Pb . The experimental levels of ^{210}Pb ¹¹ and ^{206}Pb ¹² are shown in Figs. 1 and 6. We have repeated the previous calculations with E_{α_1} and E_{α_2} in Eq. (10) replaced by these experimental phonon energies, again using the Herling-Kuo interactions to calcu-

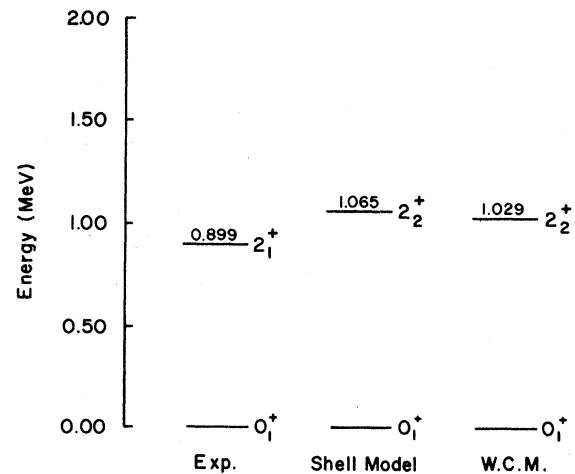


FIG. 9. Excitation spectrum of ^{204}Pb . The experimental phonon energies are used in the W. C. M.

late mixing matrix elements. The results are shown in Figs. 8 and 9 for ^{212}Pb and ^{204}Pb , respectively. Compared to the experimental levels,¹³ the 2_1^+ and 4_1^+ shell-model states of ^{212}Pb are low in energy. The use of experimental phonon energies in the weak-coupling model pushes the 2_1^+ state up to the right energy, but the 4_1^+ state is pushed up too far. For ^{204}Pb , the excitation of the shell-model 2_1^+ state relative to the ground state is larger than the experimental value.¹⁴ With experimental phonon energies the excitation of the 2_1^+ state is smaller, but not enough so.

4. CONCLUSIONS

We have applied a series of weak-coupling-approximation schemes to the calculation of wave functions and energy levels for the nuclei ^{204}Pb and ^{212}Pb . These results have been compared with exact shell-model calculations. We have found that the properties of many of the low-lying states are very accurately reproduced with small-dimension weak-coupling models. The weak-coupling wave functions are much more amenable to simple physical interpretations than the rather complicated

large shell-model wave functions. The models are formulated so that much of the input can be taken directly from experiment, which makes further application of similar models in this mass region particularly interesting.

A major difficulty in the weak-coupling model is to determine how many states should be included in the weak-coupling Hilbert space. For simplicity, the number of such states should be as small as possible. But then the resulting eigenstate in the weak-coupling model may be spurious in the sense that it does not correspond to any exact shell-model state. As shown in Fig. 3, we have found that when the eigenvalues of the weak-coupling model agree well with the exact shell-model eigenvalues, they are very insensitive to the increase of the dimension of the weak-coupling Hilbert space. Thus as an empirical rule it is necessary to vary the number of phonon states included in the weak-coupling model and retain only those eigenstates whose eigenvalues are insensitive to this variation.

We thank Dr. G. E. Brown, Dr. A. Arima, Dr. G. H. Herling, and Dr. M. Ichimura for many helpful discussions.

APPENDIX

In this Appendix, we discuss how we evaluate the overlap of weak-coupling wave functions with exact shell-model wave functions.

Let the wave functions obtained from the weak-coupling model and the shell model be

$$|w\rangle = \sum_{\alpha} d_{\alpha w} |\alpha\rangle$$

and

$$|s\rangle = \sum_{\xi} g_{\xi s} |\xi\rangle,$$

respectively. In the above, $|\alpha\rangle$'s are the normalized two-phonon states which have already been discussed in Sec. 2; $|\xi\rangle$'s are the shell-model basis states and have the following general form:

$$|\xi\rangle = \frac{1}{\sqrt{N_{\xi}}} |(j_1^{n_1} v_1 \alpha_1 J_1) \cdots (j_r^{n_r} v_r \alpha_r J_r)^{J'_r} (j_s^{n_s} v_s \alpha_s J_s)^{J'_s} \cdots (j_m^{n_m} v_m \alpha_m J_m) J\rangle, \quad (\text{A2})$$

where the single-shell state $|(j_s^{n_s} v_s \alpha_s J_s)^{J'_s}\rangle$ has n_s particles in orbit j_s and is described by seniority v_s , angular momentum J_s , and an extra quantum number α_s which is needed when there is more than one single-shell state with the same n_s , v_s , and J_s . J'_s is the subtotal angular momentum, i.e., the resultant of J'_r and J_s . N_{ξ} is the normalization factor of the shell-model basis state. For the case of ^{212}Pb or ^{204}Pb , we have $n_1 + \cdots + n_m = 4$. Then there are five distinct classes of basis states, namely

- (1) $|j_a^4 v_a \alpha_a J\rangle,$
- (2) $|(j_a^3 v'_a \alpha'_a J'_a) j_b J\rangle,$
- (3) $|(j_a^2)^{J'_a} (j_b^2)^{J'_b} J\rangle,$
- (4) $[[(j_a^2)^{J'_a} j_b]^{J'_b} j_c J\rangle,$
- (5) $[[(j_a j_b)^{J'_b} j_c]^{J'_c} j_d J\rangle.$

To calculate the overlap of shell-model wave functions with weak-coupling wave functions, we found it convenient to express $|\xi\rangle$ in terms of the form $|(ab)^{J_1} (cd)^{J_2} J\rangle,$

$$|\xi\rangle = \sum_{J_1 J_2} h_{\xi}^{J_1 J_2} |(ab)^{J_1} (cd)^{J_2} J\rangle. \quad (\text{A4})$$

The transformation coefficients $h_{\xi}^{J_1 J_2}$ can be easily obtained. From Eq. (A3), we have

$$\begin{aligned}
 (1) \quad |j_a^4 v_a \alpha_a J\rangle &= \sum_{J_a'' J_a'''} \sum_{v_a' \alpha_a' J_a'} (j_a^3 v_a' \alpha_a' J_a'; j_a | \{ j_a^4 v_a \alpha_a J \} \\
 &\quad \times (j_a^2 v_a'' \alpha_a'' J_a''; j_a | \{ j_a^3 v_a' \alpha_a' J_a' \} U(J_a'' j_a J j_a'; J_a' J_a''') | (j_a j_a)^{J_a''} (j_a j_a)^{J_a''' } J), \\
 (2) \quad |(j_a^3 v_a' \alpha_a' J_a') j_b J\rangle &= \sum_{J_a'' J_a'''} (j_a^2 v_a'' \alpha_a'' J_a''; j_a | \{ j_a^3 v_a' \alpha_a' J_a' \} U(J_a'' j_a J j_b; J_a' J_a''') | (j_a j_a)^{J_a''} (j_a j_b)^{J_a''' } J), \\
 (4) \quad |[(j_a^2)^{J_a''} j_b]^{J_b} j_c J\rangle &= \sum_{J_c} U(J_a'' j_b J j_c; J_b J_c) | (j_a j_a)^{J_a''} (j_b j_c)^{J_c} J), \\
 (5) \quad |[(j_a j_b)^{J_b} j_c]^{J_c} j_a J\rangle &= \sum_{J_a} U(J_b j_c J j_a; J_c J_a) | (j_a j_b)^{J_b} (j_c j_a)^{J_a} J),
 \end{aligned} \tag{A5}$$

where $(\dots | \{ \dots \})$ and $U(\dots)$ are, respectively, the coefficients of fractional parentage and the Racah coefficients. Then the overlap between $|w\rangle$ and $|s\rangle$ is given by

$$\begin{aligned}
 \langle s | w \rangle &= \sum_{\xi} \sum_{\alpha} \sum_{J_1 J_2} \sum_{(ef)} \sum_{(gh)} \frac{1}{\sqrt{N_{\xi}}} \frac{1}{\sqrt{N_{\alpha}}} g_{\xi s} d_{\alpha w} h_{\xi}^{J_1 J_2} \\
 &\quad \times \frac{A_{\alpha_3}^{(ef)}}{(1 + \delta_{ef})^{1/2}} \frac{A_{\alpha_4}^{(gh)}}{(1 + \delta_{gh})^{1/2}} \langle (ab)^{J_1} (cd)^{J_2} J | (ef)^{J_3} (gh)^{J_4} J \rangle,
 \end{aligned} \tag{A6}$$

where the four-particle overlapping matrix element can be evaluated according to Eq. (3) in Sec. 2.

[†] Work supported by the U. S. Atomic Energy Commission.
^{*} Research sponsored in part by U. S. Atomic Energy Commission under contract with Union Carbide Corporation.
¹ A. Arima, H. Horiuchi, and T. Sebe, *Phys. Lett.* **24B**, 129 (1967).
² A. Arima and V. Gillet, *Ann. Phys.* **66**, 117 (1971).
³ A. D. Jackson, T. T. S. Kuo, and J. D. Vergados, *Phys. Lett.* **30B**, 455 (1969).
⁴ A. Arima and I. Hamamoto, *Ann. Rev. Nucl. Sci.* **21**, 55 (1971).
⁵ S. K. M. Wong and A. P. Zuker, *Phys. Lett.* **36B**, 437 (1971).
⁶ A. Bohr, in *Proceedings of the International Symposium*

on Nuclear Structure, Dubna, 1968 (International Atomic Energy Agency, Vienna, Austria, 1969), p. 179.
⁷ P. O. Lowdin, *Rev. Mod. Phys.* **30**, 259 (1967).
⁸ G. H. Herling and T. T. S. Kuo, *Nucl. Phys.* **A181**, 113 (1972).
⁹ G. H. Herling and T. T. S. Kuo, Naval Research Laboratory Report No. 2258, 1971 (unpublished).
¹⁰ T. T. S. Kuo, S. Y. Lee, and K. F. Ratcliff, *Nucl. Phys.* **A176**, 65 (1971).
¹¹ M. B. Lewis, *Nucl. Data* **B5**(No. 6), 631 (1971).
¹² K. K. Seth, *Nucl. Data* **B7**(No. 2), 161 (1972).
¹³ S. C. Pancholi and M. J. Martin, *Nucl. Data* **B8**(No. 2), 165 (1972).
¹⁴ M. J. Martin, *Nucl. Data* **B5**(No. 6), 601 (1971).